Heliyon 10 (2024) e40681

Contents lists available at ScienceDirect

Heliyon

journal homepage: www.cell.com/heliyon

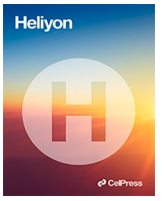

Research article

Performance evaluation of innovative self-healing corrosion protection coatings for prestressing strands

Roz-Ud-Din Nassar [a,*], Kadhim Alamara [b], Anagi Balachandra [c], Parviz Soroushian [d], Tewodros Ghebrab [e]

[a] Department of Civil and Infrastructure Engineering, American University of Ras Al Khaimah, Ras Al Khaimah, United Arab Emirates
[b] Department of Mechanical and Industrial Engineering, Liwa College, Abu Dhabi, United Arab Emirates
[c] Research Development, College of Engineering, University of Michigan, USA
[d] Emeritus of Civil and Environmental Engineering Department, Michigan State University, USA
[e] Department of Civil, Environmental, and Construction Engineering, Texas Tech University, USA

ARTICLE INFO

Keywords:
Prestressing tendons
Corrosion
Corrosion protection
Self-healing
Concrete
Bond strength

ABSTRACT

This study presents the design and experimental evaluation of advanced corrosion protection coatings for application on prestressing strands which are the core constituents of prestressed concrete structures such as bridges. Variety of self-heal coatings embodying corrective and protective phenomena in response to the degrading effects of corrosion have been designed and tested in simulated aggressive weathering conditions. Standard 7-wire prestressing strands coated with self-heal epoxy, self-heal toughened epoxy and hybrid epoxy coating systems were subjected to salt fog spray up to a duration of 2500 h, and 3M $CaCl_2$, 3M NaOH, saturated $Ca(OH)_2$ solutions and distilled water up to 45 days duration. Furthermore, rust creepage of the coated prestressing strands was measured after extended exposure to aggressive corrosive environment. Bond strength of the self-heal epoxy coated prestressing strands was evaluated through pullout test using high-strength concrete.

Significant improvement in corrosion resistance, hydrolytic stability, marked reduction in rust creepage, and improved bond strength, brought about by the innovative self-heal epoxy coatings were recorded in laboratory tests. Furthermore, electrochemical impedance spectroscopy (EIS) data proved excellent corrosion protection qualities of self-healing coatings. The ATR-FTIR spectra of various self-heal epoxy coating systems and optic microscopic images of the coatings further verified these findings.

1. Introduction

The distinct structural advantages of prestressed concrete have led to a consistent rise in its share of infrastructure systems in the United States over the past few decades [1,2]. Prestressing strands are the core saturated constituents of prestressed concrete structures. Exposed prestressed concrete structures (e.g., bridges), are vulnerable to corrosion, the high stresses induced in the prestressing strands in service enhance its chances [3–10]. The potential for split microcracking/cracking of concrete along the transfer length of

* Corresponding author.
E-mail addresses: rozuddin.nassar@aurak.ac.ae (R.-U.-D. Nassar), kadhim.alamara@lc.ac.ae (K. Alamara), anagi4248@outlook.com (A. Balachandra), parvizsoroushian1@gmail.com (P. Soroushian), tewodros.ghebrab@ttu.edu (T. Ghebrab).

https://doi.org/10.1016/j.heliyon.2024.e40681
Received 1 August 2024; Received in revised form 31 October 2024; Accepted 22 November 2024
Available online 23 November 2024

strands compromises the protection provided by concrete [11]. Considering the all-important role of strands in prestressed concrete structures, their corrosion has serious safety and life-cycle cost implications [12]. In spite of the commercial availability of a range of corrosion-resistant prestressing strands (epoxy-coated, metal-clad, galvanized, etc.), conventional (black) strands have retained a dominant share of the prestressing steel markets [13–16]. The high cost and some enduring technical concerns have dampened the market appeal of existing corrosion-resistant prestressing strands [17].

Corrosion of steel is a common concern across diverse disciplines. There has been considerable progress during the recent years towards development of new corrosion protection coating and alloying strategies [18,19]. These new strategies provide powerful tools for overcoming the economic and technical drawbacks of today's corrosion-resistant prestressing strands. The advanced corrosion protection strategies selected based on performance and cost considerations for evaluation in the Phase I of this work include: (i) composition-modulated multilayered polymer or metal coatings embodying complementary corrosion protection mechanisms; (ii) hybrid organic-inorganic coatings with synergistic contributions of different constituents towards corrosion protection;

(iii) self-heal coatings; (iv) inorganic coatings with favorable cost structure and sustainability; (v) polymer nanocomposite coatings for reliable and cost-effective corrosion protection; (vi) chemically modified epoxy coatings with improved damage resistance, stability and adhesion capacity; and (vii) intrinsically conductive polymer coatings providing corrosion protection via reversible electroactive phenomena.

Self-healing materials have an intrinsic capability to mobilize their resources or modify their structure in response to the damaging phenomena in order to repair or compensate for the damaging effects [20]. Self-healing features could also be mobilized to prevent catastrophic growth of critical defects which evolve in structural materials during manufacturing and in service [21,22]. Self-healing materials when used as coatings exhibit qualities to mobilize local corrective/protective phenomena in response to damaging effects (e.g., scratching) which expose the steel surface to corrosive environments [23]. Epoxy coatings can assume self-heal qualities through complementary use of selected corrosion inhibitors and conductive polymer constituents [24–26]. The self-heal qualities of the coating benefit from the improvements in strain capacity and toughness imparted by chemical modification of the epoxy with a silicone. Unlike silane (used in conventional epoxy), silicone has no methoxy groups; hence, the refined epoxy has no volatile emissions, and provides improved durability characteristics. A key compound which enables development of self-heal coatings is zinc phosphate [27–29]; it is a green (safe, environmentally friendly) additive, unlike some toxic compounds, e.g. chromate pigments, which can be easily incorporated into epoxy coatings. Past investigations have indicated that zinc phosphate renders self-healing effects by covering steel substrate with an insulating film at damaged areas. The corrosion inhibiting effects of zinc phosphate beneath the scratched areas of coatings might be the effect of development of a protective phosphatisation salt layer on the exposed steel surface. This layer consists of $Fe{+}3O(OH)$, $Fe(OH)_3$ and $Fe_2(PO_4)(OH)$ [29]. In addition to phosphatisation of the iron surface, zinc phosphate also forms compounds with the carboxyl and hydroxyl groups of the binder in coating [28], and improves the barrier qualities of the coating [30].

Complementary use of different additives is considered in development of self-heal organic coatings. In order to improve the resistance of organic coatings against the penetration of water, oxygen and aggressive ions, different anti-corrosion additives have been formulated and made part of coating matrix. Some of these additives impart protective qualities via electrochemical mechanisms. Such additives (which tend to be soluble in water) are also referred to as inhibitors. Zinc chromate and red lead are two typical inhibiting additives [31]; they are, however, toxic. Zinc phosphate impart self-healing characteristic by creating a protective layer on the steel surface at damaged locations. As noted earlier, the corrosion inhibiting effects of zinc phosphate beneath the scratched areas of coatings might be due to the formation of a phosphatisation salt-based film that protects the exposed steel surface, and formation of compounds with the carboxyl and hydroxyl groups of binder which improve the barrier qualities of the coating.

This investigation focusses on the formulation and experimental evaluation of self-healing corrosion protection coating methodology for production of corrosion-resistant prestressing strands that will address key market needs. Chemical resistance, water resistance, damage resistance, and corrosion protection characteristics of the refined epoxy coatings developed in this study have been evaluated in aggressive environments per the guidelines of the relevant ASTM standards. The new corrosion-resistant coating is devised to address the shortcomings of existing systems in terms of resistance against rust creepage, damage resistance, and bond strength to concrete and steel.

Fig. 1. Uncoated (bare) seven-wire (low relaxation) prestressing strand.

2. Materials

2.1. Prestressing strands

A view of the 7-wired, 13 mm diameter, Grade 270 prestressing strand used in the experimental investigation is shown in Fig. 1. Table 1 presents the properties of this prestressing strand.

2.2. Self-healing epoxy coatings

Self-heal qualities of the innovative coatings enable the mobilization of local corrective/protective phenomena in response to various damaging effects, and thus protect the steel surface in corrosive environments. Five classes of self-healing epoxies designated as; (i) *Self-healing epoxy* (ii) *Self-Healing Toughened Epoxy I* (iii) *Self-Healing Toughened Epoxy II* (iv) *Self-Healing Toughened Epoxy III* and (v) *Hybrid Epoxy Coating*, were developed and evaluated in this research program.

The development of basic self-healing epoxy coating system involved the use of epoxy resin (Part-A) and hardener which comprised of epoxy curing agent modified Polyamide (Part-B). Furthermore, Talc was incorporated in Part-A to reduce moisture/oxygen permeation and Zinc Phosphate as anti-corrosion Pigment. Parts A & B were homogeneously mixed at the weight ratio of 1:1.28 and degassed prior to coating application. The self-healing toughened epoxy-I incorporates a reactive amine functional silicone which acts as a cross-linker to improve the physical properties and the long-term performance of the coating system, in addition to the above stated basic composition of self-healing epoxy. The composition of self-healing toughened epoxy-II is similar to that of self-healing toughened epoxy-I except that a small amount of Cerium nitrate was added to Part-A by dissolving it in Xylene to yield a concentration of 1×10^{-3} M. Similarly, self-healing toughened epoxy-III incorporates conductive polyaniline (PANI) to the basic composition of self-healing epoxy to improve its damage resistance, bonding and barrier qualities. The hybrid epoxy coating system on the other hand embodies a combination of the features, such as: (i) nanocomposite for enhancing barrier qualities, scratch and abrasion resistance, and adhesion qualities; (ii) basic self-healing formulation for damage resistance and durability. This composition results in toughening effects for enhancing flexibility to allow for bending/winding during handling and prestressing. Further details on the composition, constituent characteristics, and weight proportions of the five types of coatings may be found in elsewhere [32].

Figs. 2 and 3 show the visual appearances and optic micrographs of the 7-wire prestressing strand before and after coating with different self-heal epoxy systems, respectively.

2.3. High-strength concrete

High-strength concrete (HSC) which is characterized by its high strength, enhanced microstructure characteristics, higher moisture barrier attributes, and longevity of service life has been increasingly used for the construction of civil infrastructure, such as prestressed concrete bridges. Accordingly, HSC was used in this study to prepare the strand pullout test specimens. Table 2 presents the mixture design of the HSC used in the experimental program.

3. Methods

3.1. Attenuated Total Reflectance Fourier Transform infrared spectroscopy (ATR-FTIR)

ATR-FTIR tests were performed in order to gain insight into the chemical structure of different epoxy coating systems. AFT-FTIR is a powerful nondestructive test technique for investigation of surface coatings. ATR uses the reflectance of the sample; an attenuated total reflection measures the change in a totally internally reflected infrared beam when the beam comes in contact with the sample. The infrared beam hits an optically dense crystal (i.e. diamond or germanium), which then creates an evanescent wave that subsequently protrudes the sample (0.5–5 μm). In regions where sample absorbs energy, the alteration of the evanescent wave will be detected. In this investigation the ATR-FTIR measurements were carried out on a JASCO FTIR-4100 spectrometer equipped with an Attenuated Total Reflectance (ATR) accessory. Evolution of the FTIR spectra of epoxy coatings applied to strands was monitored under different exposure conditions. Scans were performed at a resolution of 1 cm^{-1}.

Table 1
Properties of low-relaxation prestressing strands.

Grade	Nominal Diameter (mm)	Strand Tolerance (mm)	Minimum Breaking Strength (kg)	Minimum Yield Strength at 1 % Extension (kg)	Minimum Elongation	Nominal Weight (kg/1000 m)
270 K	12.7	13.35/12.55	18, 733	16,860	3.5 %	775
Relaxation Properties						
Initial Stress		Maximum Relaxation after 1000 h.				
70 % G.U.T.S.		2.5 %				
80 % G.U.T.S.		3.5 %				

Fig. 2. Photographs of prestressing strands: (a) uncoated; (b) self-healing epoxy (c) self-healing/toughened epoxy-I; and (d) hybrid self-healing epoxy.

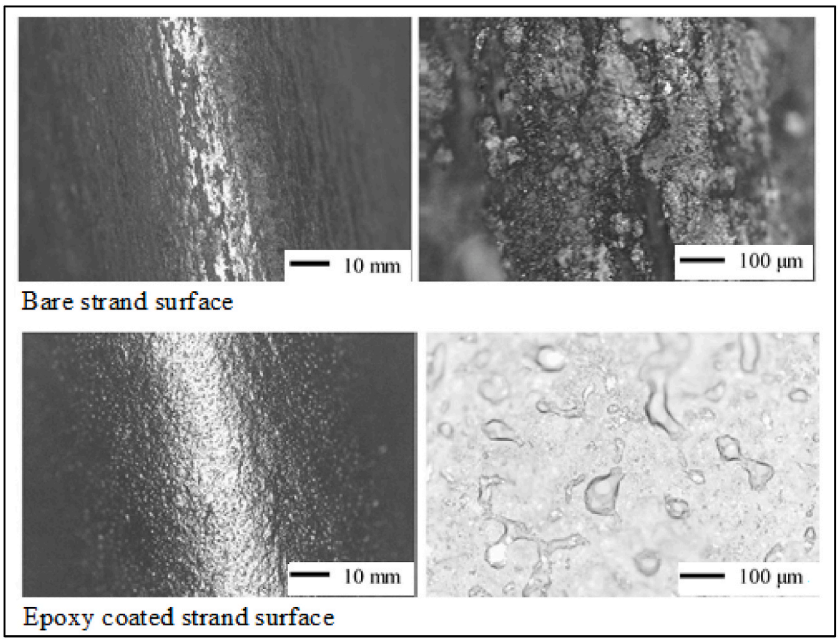

Fig. 3. Optic micrographs of the coated and uncoated strand surfaces at two different magnifications.

Table 2
Mixture design of HSC.

Mixture Component	Mass proportion
Ordinary Portland	1
Silica Fume	0.12
Sand (0 – 2.00 mm)	2.58
Coarse aggregate (9.5 mm)	2.62
Water	0.40
High-range water reducer	0.018

3.2. Salt fog spray test

This test is a standardized method for checking the corrosion resistance of coatings under exposure to aggressive environments. This is an accelerated corrosion test that allows for determining the corrosion tolerance of coated samples under exposure to salt fog

spray following ASTM B117 (Standard Practice for Operating Salt Spray (Fog) Apparatus) [33]. Coated specimens were placed in a salt fog spray cabinet (Fig. 4) at a controlled temperature of 35 °C ± 1 °C. The specimens were monitored periodically in order to detect any rust formation or change in the coating appearance. Salt fog was produced in this chamber via nebulization of 5 m% NaCl aqueous solution. Observations for signs of corrosion were made periodically (every 250 h). In order to ensure adequate corrosion resistance, after 3000 h of exposure, no evidence of rust shall be present, and the specimens shall be holiday-free per ASTM standard A882 "Standard Specification for Filled Epoxy-Coated Seven-Wire Prestressing Steel Strand" [34]. Deterioration conditions of different coating systems were also evaluated based on the level of blistering detected in the coating according to ASTM D714 (Standard Test Method for Evaluating the Degree of Blistering of Paints) [35].

3.3. Electrochemical impedance spectroscopy (EIS)

EIS is a non-destructive technique which provides accurate kinetic and mechanistic information relevant to the corrosion resistance of a system that is susceptible to corrosive effects [36,37]. EIS is a well-known electrochemical means of evaluating the performance of organic coatings; it is a powerful tool for evaluation of corrosion rate. The impedance technique has been successfully used in a range of fields to investigate the performance of coating systems under exposure to highly corrosive environments. Particularly, it has been useful in investigating the performance of organic coatings at the locations of pores and defects.

The impedance of different coating systems was measured using an electrochemical instrument equipped with a potentiostat. This technique involves application of alternating current signal of a minor magnitude into the body of material over a wide range of frequencies, and measuring the responding current and its phase angle shift. The output from the EIS instrument is an impedance spectrum of the material, typically ranging between 100,000 and 0.01 Hz. The equivalent circuit modelling technique is used to analyze EIS data for gauging the deterioration of coatings at metal/coating interface.

The EIS test conditions were tailored to simulate corrosion of steel in the alkaline environment of concrete exposed to salt solution. Fig. 5 shows the EIS test setup used in this experimental program. Periodic impedance measurements were made with the coated samples under sustained exposure to 0.1 M NaCl in saturated $Ca(OH)_2$ solution (pH13) (Fig. 5 (b)). The EIS tests were conducted using a CHI660D (USA) workstation with a three-electrode system (Fig. 5a). In this test, the coated sample acts as the working electrode. A saturated calomel electrode (SCE) was used as the reference electrode, and a stainless-steel sheet as the counter electrode (Fig. 5(b) and (c)). Impedance tests on coatings were performed using the potentiostat system at open circuit potential, with ±10 mV excitation from 100 kHz to 0.01 Hz. The impedance measurements were made on coated prestressing strands prior to aging and after different periods of exposure to salt fog spray.

3.4. Measurement of rust creepage

The guidelines of ASTM D1654 "Evaluation of Painted or Coated Specimens Subjected to Corrosive Environments" [38], were used to measure the intensity of rust creepage at the scribe location. Scribe measuring 76 mm in length was made on the coating across the specimen >1.25 cm away from its edges. The scribe was made using a scribing tool which produces a uniform cut through the coating. This scribe meets the requirements of having an adequate length to cover a significant test area, and not contacting the specimen edges. The scribe penetrates through the coating on metal, leaving a uniform bright line.

Coated specimens having scribe-damage on them were tested as per the guidelines of ASTM B117. The maximum and minimum creepage from the scribe were recorded, and it was noted whether or not the maximum was an isolated spot. The mean width of corrosion zone was obtained as the average of 6 measurements. These measurements were made at locations that were uniformly distributed along the scribe length, ignoring 3 mm segments at both ends of the scribe. The resulting arithmetic mean width (w_c) and the original width (w) of scribe were used to calculate rust creepage (c) using equation-1 below:

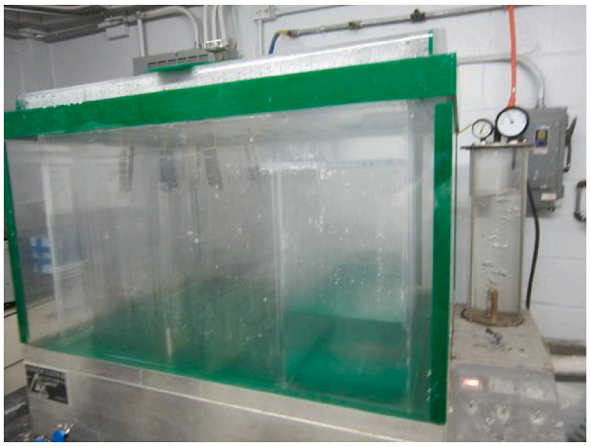

Fig. 4. The salt fog spray apparatus (ASTM B117) used in the project.

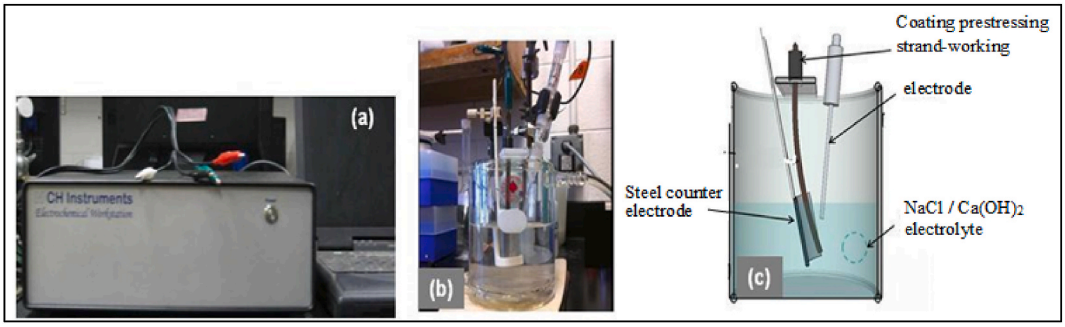

Fig. 5. (a) EIS set-up (CH Instrument CHI660D Electrochemical Analyzer), (b) and (c) the three-electrode cell used in EIS experiments.

$$c = \frac{(w_c - w)}{2} \tag{1}$$

3.5. Monitoring of self-healing

Cured epoxy-coated steel sheet samples were scratched (making a cross) at the center using a TiC tip pen in order to introduce a controlled damage on the coating. Corrosion performance of the coating was examined after exposure to 3.5 % NaCl solution over specific time periods. The coating performance was monitored using EIS as described in Section 3.3. EIS is ideally suited for determining the performance of protective organic coatings on metals. EIS measurements were made with the coated sample acting as the working electrode. In this case too, SCE was the reference electrode, and a stainless-steel sheet as counter electrode. Tests on coatings were performed at open circuit potential, with ±10 mV excitation at frequencies ranging from 100 kHz to 0.01 Hz. Care was taken to keep the exposed area constant at 11.25 cm^2 covering the cross for all samples, with the cross placed in the middle of the exposed measurement area.

3.6. Chemical and water resistance

3.6.1. Chemical resistance

Coated samples were immersed in a solutions of 3M $CaCl_2$, 3M NaOH and saturated $Ca(OH)_2$ in distilled water at 20 ± 1 °C for 45 days per ASTM G-20 [39] (Fig. 6). Before and after immersion, coatings were inspected in order to detect any blistering, softening, loss of bond or holidays.

3.6.2. Water resistance

The hydrolytic stability of coatings is an important parameter from the stand point of anticorrosive application. For evaluating hydrolytic stability, coated samples were immersed in 20 ± 1 °C distilled water for 45 days per ASTM G-20 [39]. Before and after immersion, coatings were inspected for detection of any blistering, softening, loss of bond or holidays in coating.

3.7. Bond strength of prestressing strands to concrete

Following the procedure reported in literature [40], the pullout test on the prestressing strand was carried out. Fig. 7 shows the schematics and test setup of the pullout test. Epoxy coating (hybrid epoxy coating in this case) was applied via electrostatic spray to individual wires in the course of their helical winding into seven-wire strand. Keeping the bonded length equal to twice the bar diameter, the non-bonded length of the bar was sheathed with PVC pipe according to the guidelines of the test. A servovalve-controlled hydraulic test system was used to apply the pullout load at a displacement rate of 0.5 mm/min. Two LVDTs were used to measure bond slip between the bar and concrete at the loaded and free ends of the bar.

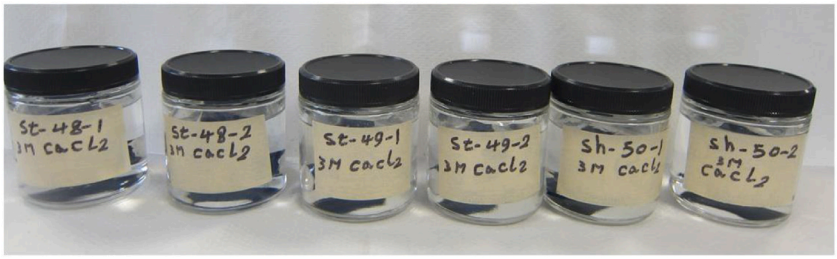

Fig. 6. Chemical resistance tests on different coating systems.

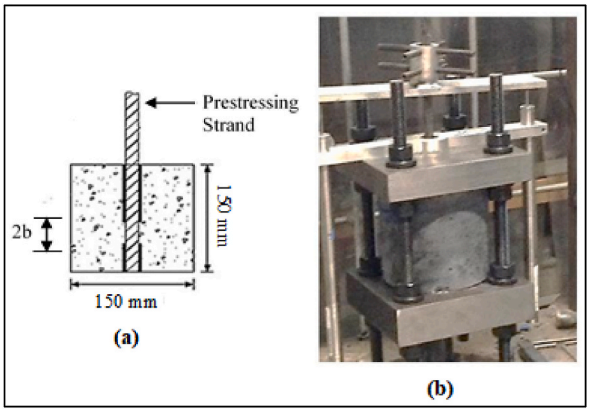

Fig. 7. Pullout test: *(a)* specimen *(b)* test setup.

4. Results and discussions

4.1. ATR-FTIR spectra of self-healing coatings

Fig. 8 presents the ATR-FTIR spectra obtained for various self-healing epoxy coatings applied on prestressing strands. The characteristic peaks of the primary chemical functional groups such as the methyl groups (2850 cm^{-1}), phenyl groups (1610 cm^{-1} and 1510 cm^{-1}) and ether bonds (1230 cm^{-1} and 1040 cm^{-1}) of epoxy systems, are seen in these spectra [41,42]. In addition, the characteristic bands associated with stretching and bending vibration of Si-O-Si at 1108 cm^{-1} and 817 cm^{-1}, corresponding to silica, are observed in the spectra. Furthermore, bands at 700-780 cm^{-1} and 1200-1300 cm^{-1} are observed due to P-O-P bridge vibrations, indicating successful incorporation of zinc phosphate into the coating structure.

Several sharp absorption bands from 900 to 1200 cm^{-1} are also observed due to stretching of the PO_4^{3-} group [43].

Reaction of epoxy with silicone amine to impart toughening effects can be verified using the FTIR spectra of self-heal toughened epoxy. Si-CH_3 groups are recognized by a strong, sharp band at about 1261 cm^{-1} together with a band in the 750-865 cm^{-1} range. The

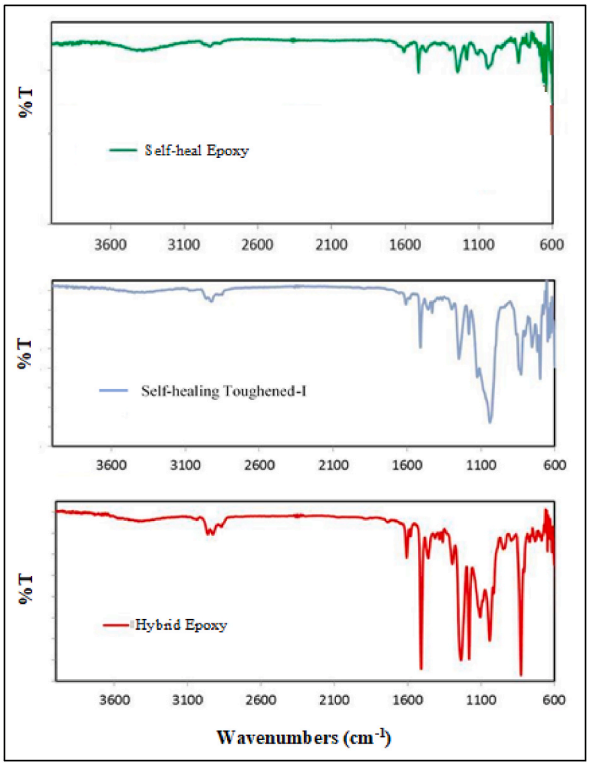

Fig. 8. ATR-FTIR spectra of self-heal, self-heal toughened-1 and hybrid epoxy coating systems.

strong infrared bands in the region 1000-1130 cm^{-1}, providing further indications for the presence of Si-O-Si bonds. These observations confirm that the reaction of self-healing epoxy with silicone amine has been successful.

The hybrid epoxy FTIR spectra indicate that this coating exhibit bands originating from both the nanocomposite and self-heal functionalities along with those associated with the toughening effects. One can thus anticipate that the hybrid epoxy coating would offer superior performance characteristics when compared with epoxy coatings embodying individual functional features.

4.2. EIS examinations

EIS was used to examine the differences in corrosion activity between plain and coated prestressing strands. Generally, a higher impedance modulus (/Z/) at the lower-frequency range in the Bode plot indicates a more effective corrosion protection, and the shape of the Nyquist plot provides an indication of the coating impedance behavior. The bare seven-wire prestressing strand (inset in Fig. 9) had a/Z/value of about 10^2 Ω cm^2 at low frequencies. With the (self-heal) Epoxy Type II coating, the/Z/value increased by five to seven orders of magnitude to 10^7–10^9 Ω cm^2 at the same frequency (Fig. 9). The high value of/Z/at low frequencies points at the very low porosity and defect concentration of the (self-heal epoxy) coating, which are indicative of excellent corrosion protection qualities [44]. The larger semicircle (or in some cases the straight line parallel to $Z_{imaginary}$) in impedance plots point at the improved corrosion protection qualities. Scully and Hensley [45] suggest that the coating resistance needs to be at least 10^7 Ω cm^2 for effective protection of metal substrates.

The Bode plots for various types of self-heal epoxy coated prestressing strands are shown in Fig. 10. The EIS data in Fig. 10 reflects the effect of corrosion protection qualities of the self-healing. The self-heal coating increases the oxide layer thickness, promotes adhesion, and also facilitates development of better coating barrier qualities for more effective corrosion protection. Some coatings produced impedance values >10^7 Ω cm^2, which point at the enhanced corrosion resistance qualities. It is also important to note that coatings with very high impedance values (>10^8 Ω cm^2) generate noise in Bode plots at lower frequencies due to the lower signal-to-noise (S/N) ratios.

The impedance of different coatings was monitored in a simulated concrete environment in order to evaluate the corrosion protection qualities of different coating systems. The EIS test conditions were tailored to simulate corrosion of coated strands in the alkaline environment of concrete exposed to salt solution. For this purpose, periodic impedance measurements were made with the coated strands exposed to NaCl solution (of 0.1 Molality) in a saturated $Ca(OH)_2$ solution. Table 3 shows the impedance values recorded at the lowest frequency for various epoxy coating formulations applied to prestressing strands prior to salt fog exposure. For comparison, a control epoxy coating system was also evaluated in application to prestressing strands.

As noted earlier, higher impedance values and lower absolute values of (negative) potential are indicative of better corrosion protection qualities. All modified epoxy systems provided lower negative potentials when compared with the standard corrosion protection epoxy coating. The hybrid (self-healing/nanocomposite/toughened) epoxy stood out among the other types of coatings. It provided impedance values that are two orders of magnitude greater than those provided by the control epoxy, pointing at its significantly improved performance. Hence the impedance measurements were made on the hybrid epoxy coated prestressing strands after different periods of exposure to salt fog spray.

The extent of damage to the corrosion protection coatings applied to prestressing strands correlates with the drop in impedance relative to the initial value. Impedance measurements for the preferred hybrid coating system are presented in Table 4 and Fig. 11 before and after various periods of exposure to salt fog spray. Test data in Table 4 points at excellent performance of hybrid epoxy

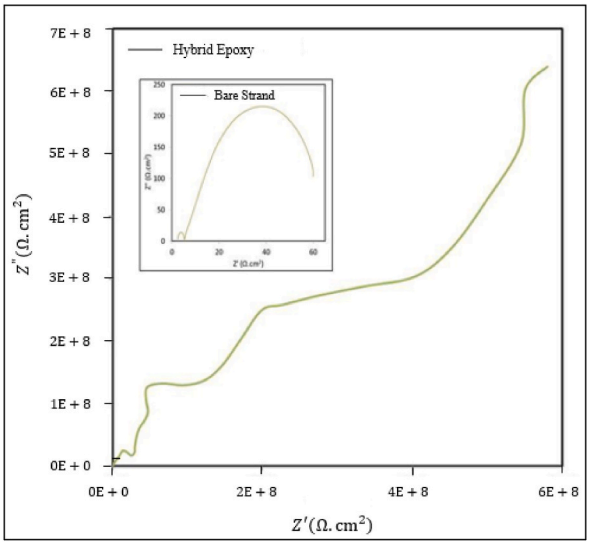

Fig. 9. Nyquist plot for bare and hybrid epoxy coated prestressing strands *(Inset shows the bare strand test data)*.

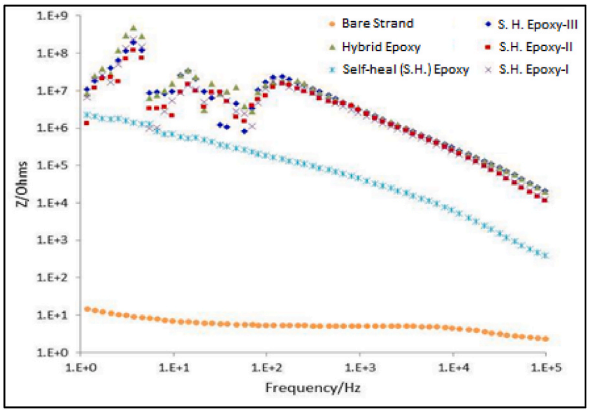

Fig. 10. Bode plots for epoxy coatings on prestressing strands measure in 0.1M NaCl/saturated $Ca(OH)_2$.

Table 3
Measured values of impedance and open circuit potential for prestressing strands with different corrosion protection coating systems.

	Coating System	Initial Impedance ($\Omega.cm^2$)	Initial Potential (V)
1	Control Epoxy	2.69E+09	−0.727
		1.35E+09	−0.774
2	Self-healing Epoxy	2.07E+09	−0.493
		2.93 E+09	−0.270
3	Self-healing Toughened Epoxy-I	9.45E+08	−0.235
		8.53E+08	−0.235
		1.78E+09	−0.241
4	Self-heal Toughened Epoxy-II (STE-II)	7.89E+09	−0.256
		1.30E+09	−0.331
5	Self-heal Toughened Epoxy-III (STE-III)	9.79E+09	−0.341
		9.95E+09	−0.356
6	Hybrid Epoxy	3.42E+11	−0.483
		2.10E+11	−0.483

Table 4
Impedance values at the lowest frequency of 0.01 Hz for hybrid coated prestressing strands measured in a simulated concrete environment under salt exposure.

Coating System	Initial		After 350H		After 700H		After 2500H
	Potential (V)	Impedance ($\Omega.cm^2$)	Potential (V)	Impedance ($\Omega.cm^2$)	Potential (V)	Impedance ($\Omega.cm^2$)	Impedance ($\Omega.cm^2$)
Hybrid Epoxy	−0.483	3.42E+11	−0.550	1.98E+09	−0.200	3.23E+09	5.31E+08
					−0.368	1.61E+09	3.36E+08
					−0.387	1.59E+09	

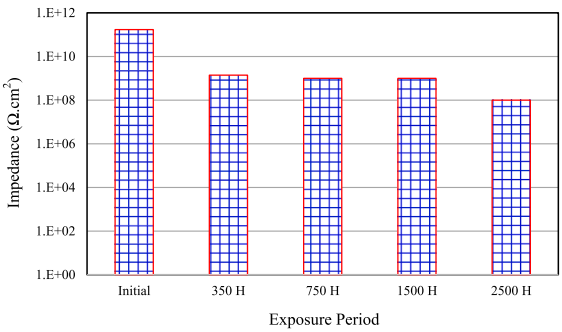

Fig. 11. Measured values of impedance for the hybrid epoxy coating system after different periods of exposure to salt fog spray.

coating in comparison to that of control epoxy system. The impedance and initial potential data of Table 4 also proves the enhanced performance of hybrid coating as compared to the other self-heal epoxy coating systems. The hybrid system offers highly desired qualities; it embodies the optimum self-healing, toughening and nanocomposite strategies.

Test results of Fig. 11 show that even after 1 month of exposure, the hybrid epoxy coating system provided a high level of impedance in the $10^9\ \Omega\ cm^2$ range. After an initial drop of about 200 times from the initial value of impedance over the first few weeks, minimal drops in impedance were observed under prolonged exposure durations. These observations indicate that the hybrid coating offers excellent corrosion protection qualities due to the combined benefits offered by different strategies for enhancement of epoxy coating systems.

4.3. Salt fog exposure

After exposure to salt fog (5 % NaCl) at 35 ± 1 °C over 2 weeks, and 1, 2 and 3 months, the exposed specimens were inspected visually for any rust formation Fig. 12 shows visual appearances of the prestressing strands with various coating systems before and after 700 and 2500 h of exposure to salt fog. It is seen that the selected coatings mitigate the rust accumulation after one month of salt fog exposure as suggested by the visual appearances in Fig. 12. On the contrary, the bare strand showed clear signs of corrosion soon after exposure to salt fog spray, which continued to grow with extended exposure. Besides visual monitoring, electrochemical impedance spectroscopy was used to monitor the performance of different coatings under extended subjection to salt fog spray.

The measured values of impedance at the lowest frequency (0.01 Hz) and open circuit potential prior to exposure to salt fog spray are presented in Fig. 13. As noted earlier, higher impedance values and lower absolute values of (negative) potential are indicative of better corrosion protection qualities. All modified epoxy systems provided lower negative potentials when compared with the standard corrosion protection epoxy coating.

Hybrid epoxy coating stand out to have the highest corrosion protection potential, followed by self-heal epoxy and self-heal toughened epoxy-I. It is noted that the hybrid system provides impedance values that are two orders of magnitude greater than those provided by the control epoxy.

4.4. Rust creepage

Fig. 14 compares the rust creepage values of different coating systems. All refined epoxy coating systems exhibited reduced rust creepage in comparison to that of control epoxy coating. The hybrid epoxy coating provided the lowest rust creepage. For self-heal and hybrid epoxy coatings, rust creepage actually decreased over longer periods of exposure to salt fog spray, which can be attributed to the self-heal qualities of these coatings.

Microscopic observations indicated that the self-heal epoxy system forms a protective layer on the surface exposed to salt fog spray. Optic microscope images of control and hybrid epoxy coatings (Fig. 15a and b, respectively) pointed at the formation of a porous rust structure at the scribe in the control epoxy coating (Fig. 15a), and a dense structure with potentially viable protective qualities in the hybrid epoxy coating (Fig. 15b).

4.5. Monitoring of self-healing qualities

In order to further evaluate the self-heal qualities incorporated into epoxy systems, comparative investigations were conducted on the control corrosion protection coating versus three classes of self-heal epoxy coatings (self-heal, self-heal/toughened epoxy-I, self-heal/toughened epoxy-II and hybrid coating systems). These coatings were applied to steel plates, which were then scratched and exposed to 3.5 % NaCl solution. Impedance and open circuit potential measurements were monitored after different immersion time periods.

Fig. 16 shows the visual appearances of scratched coatings before and after exposure to NaCl solution. The control epoxy coating exhibited more visual indications of corrosion when compared with the self-heal coating formulations. Visually, the hybrid self-heal

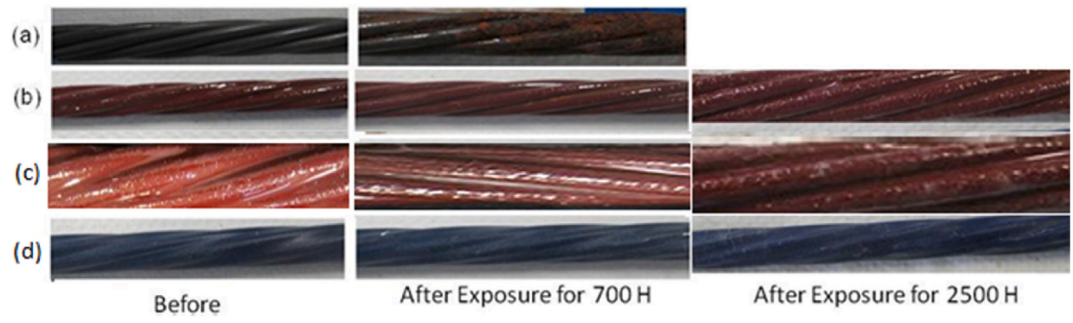

Fig. 12. Views of prestressing strands coated with various epoxy systems before and after 1 month of exposure to salt fog spray: *(a)* bare strand; *(b)* self-heal epoxy; and *(c)* self-heal toughened -I epoxy; and *(d)* hybrid (self-heal/nanocomposite/toughened) epoxy.

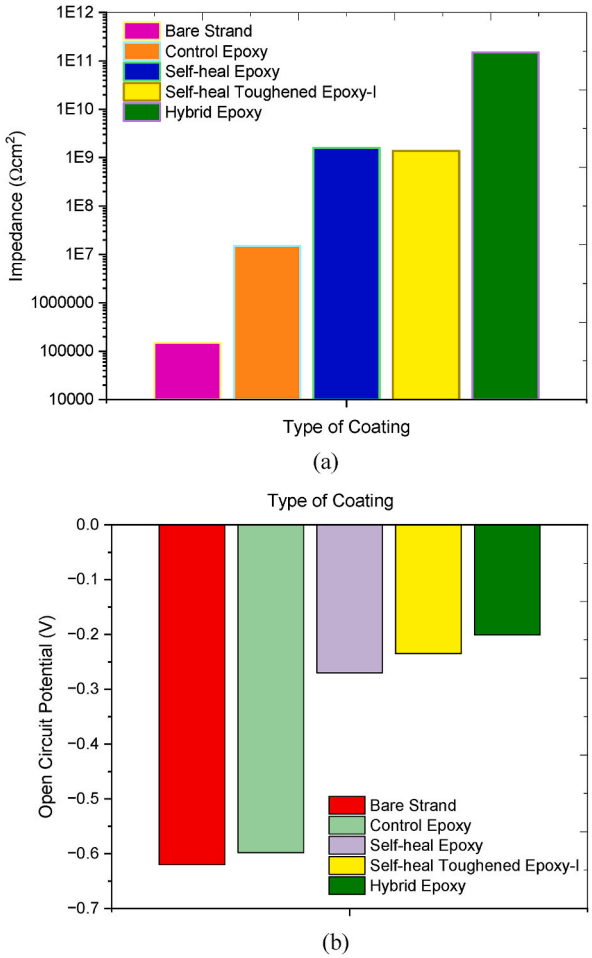

Fig. 13. Measured values: *(a)* Impedance; *(b)* Open circuit potential.

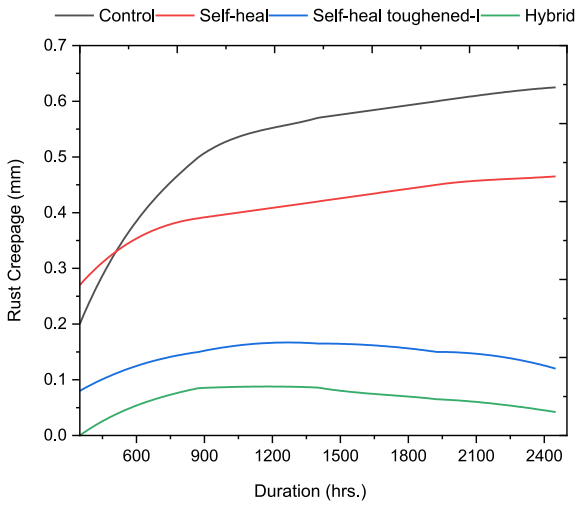

Fig. 14. Rust creepage growth versus exposure duration for different coating systems.

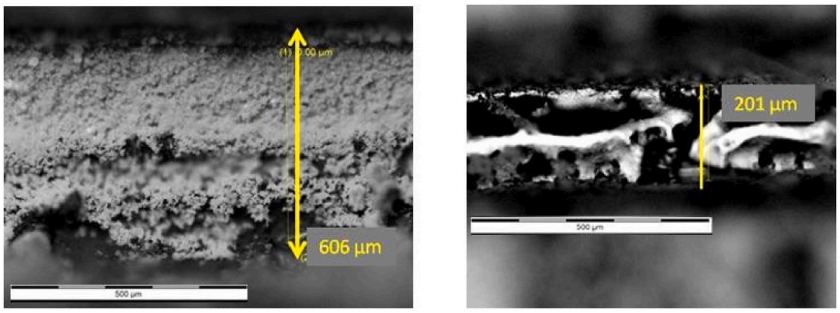

Fig. 15. Optic microscope images of control and hybrid epoxy coatings after 1 month of exposure to salt fog spray.

Fig. 16. Scratched surfaces of steel plates with different epoxy coatings before and after exposure to 3.5 % NaCl solution for 10 days.

epoxy coating appears to be in good shape after exposure of NaCl solution for 10 days. The white patch on it is probably a product of oxidation, offering good barrier qualities for corrosion protection.

4.6. Chemical and moisture resistance

Following the guidelines of ASTM G-20, hybrid epoxy coated strand samples were immersed in different solutions: (i) 3M $CaCl_2$; (ii) 3M NaOH; and (iii) saturated $Ca(OH)_2$. After Immersion for the required time periods, the coatings were inspected for any defects, blistering, softening, loss of bond or holidays. No distinct indications of damage could be detected in these series of tests.

For evaluating hydrolytic stability, coated samples were immersed in distilled water per ASTM G-20-77. Before and after immersion, coatings were inspected for detection of any blistering, softening, loss of bond or holidays. Fig. 17 shows the hybrid epoxy

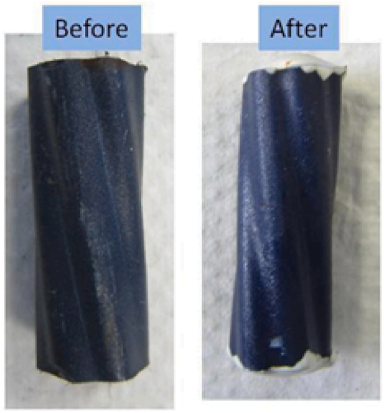

Fig. 17. Visual appearances of coating before and after immersion in water.

coated strand samples before and after immersion in water. No deboning or visual damage to the coatings could be observed. This experiment demonstrated hydrolytic stability of the hybrid epoxy coating, which is considered to be an important attribute in anti-corrosive applications.

4.7. Bond strength to concrete

Table 5 shows the test results of pullout test conducted on the bare and the hybrid (self-heal/nanocomposite/toughened) epoxy coated strands. The hybrid coated strand provided significantly higher bond strength to concrete as compared to the uncoated strand. During the pullout test, the helically wound wires which constitute the strand remained intact in the case of the coated strand, and the whole strand pulled out as one unit. This was not the case for the uncoated strand considered in this experimental work, noting that the specifics of the strand geometry (including the relatively short length considered in pullout tests) influence their failure modes. Almost no damage to the coating was caused by the de-bonding and pullout processes (Fig. 18).

5. Conclusions

In this research, broad categories of innovative corrosion protection strategies were evaluated for application to prestressing strands in order to overcome the shortcomings that have hindered broad market acceptance of corrosion-resistant strands. Diverse categories of refined epoxy coatings which embodied various self-heal, toughening and nanocomposite strategies were evaluated experimentally. The corrosion protection strategy that evolved as the preferred choice comprised a hybrid epoxy embodying selected self-heal, nanocomposite and toughening strategies applied via electrostatic powder spray on individual wires during helical winding to form the prestressing strand.

Based on the outcome of the experimental work, following conclusions are drawn.

1) Evaluation of the EIS data (measured impedance and initial potential), intermittently recorded in a simulated concrete environment to evaluate the corrosion protection qualities of various self-heal epoxy coatings applied on prestressing strands show promising performance of various types of self-heal coatings when compared with control epoxy coating in an aggressive corrosive environment. The hybrid epoxy coating stands out to be best giving initial impedance values that are two orders of magnitude higher than the other types of self-heal coatings.
2) The ATR-FTIR spectra of various types of self-heal epoxy coating systems applied on prestressing strands suggest occurrence of chemical reactions that impart toughening, enhanced barrier qualities and self-healing against damage caused by the aggressive environment.

Table 5
Pull-out test results of 7-wire prestressing strands without and with hybrid epoxy coating embedded in high-strength concrete.

Sample No.	Bare Strand		Hybrid Epoxy-Coated Strand	
	Max. Load (kN)	Bond Strength (MPa)	Max. Load (kN)	Bond Strength (MPa)
1	8.47	8.33	10.59	9.08
2	4.31	4.24	16.86	14.45
3	4.36	4.30	17.12	14.67
Average		5.6 ± 2.3		12.7 ± 3.2

Fig. 18. Visual appearances of the pulled-out prestressing strands with the hybrid epoxy coating applied via electrostatic spray to individual wires in the course of their helical winding into seven-wire strand.

3) The rust creepage growth monitored up to 2500 h show that the prestressing strands having self-healing epoxy coating systems receive the least rust creepage in comparison to that of the control epoxy specimen. The hybrid epoxy system shows the best performance in this case, too.
4) Visual appearance of the self-healing epoxy coated prestressing strand specimens after 2500 h exposure to salt fog show no signs of rust formation unlike the bare prestressing strand which showed signs of corrosion after one month of subjection to salt fog spray.
5) Self-heal epoxy-coated strands show no defects, blistering, softening or other signs of damage when exposed to variety of aggressive chemical solutions for the required period. Similarly, no signs of damage could be seen after immersion of these strands is distilled water for 45 days. These test results point at resistance of the self-heal epoxy coatings to chemical attack and moisture related degradation.
6) Compared to the bare strands, the hybrid epoxy coated strands exhibit better bond strength with concrete with no damage to coating when tested in high-strength concrete.

Funding

The research leading to these results received funding from U.S. Department of Transportation under Contract No. DTRT5714C10041. Their support is thankfully acknowledged.

CRediT authorship contribution statement

Roz-Ud-Din Nassar: Writing – original draft, Visualization, Validation, Methodology, Investigation, Formal analysis, Data curation. **Kadhim Alamara:** Writing – review & editing, Validation, Investigation, Data curation. **Anagi Balachandra:** Writing – original draft, Validation, Investigation, Formal analysis, Data curation, Conceptualization. **Parviz Soroushian:** Writing – review & editing, Supervision, Resources, Funding acquisition. **Tewodros Ghebrab:** Writing – review & editing, Validation, Investigation, Formal analysis, Data curation.

Declaration of competing interest

The corresponding author on behalf of all co-authors declares that there is no conflict of interest among them concerning this work.

References

[1] F. Kenneth, B.G.R. Dunker, Performance of prestressed concrete highway bridges in the United States- the first 40 years, PCI J. 37 (3) (1992) 48–64.
[2] F.H. Administration, Compilation and Evaluation of Results from High-Performance Concrete Bridge Projects, vol. I, U.S. Deprtment of Transportation VA, 2006. Final Report.
[3] F. Vecchi, et al., Corrosion morphology of prestressing steel strands in naturally corroded PC beams, Construct. Build. Mater. 296 (2021) 123720.
[4] M.A. Arafin, J.A. Szpunar, A new understanding of intergranular stress corrosion cracking resistance of pipeline steel through grain boundary character and crystallographic texture studies, Corrosion Sci. 51 (1) (2009) 119–128.
[5] N. Eliaz, et al., Characteristics of hydrogen embrittlement, stress corrosion cracking and tempered martensite embrittlement in high-strength steels, Eng. Fail. Anal. 9 (2) (2002) 167–184.
[6] J.R. Fernandez, Stress Corrosion Cracking Evaluation of Candidate High Strength Stainless Steels for Prestressed Concrete, 2011.
[7] W.J. Li, et al., The effects of rolling and sensitization treatments on the stress corrosion cracking of 304L stainless steel in salt-spray environment, Corrosion Sci. 68 (2013) 25–33.
[8] S.S.M. Tavares, et al., Investigation of stress corrosion cracks in a UNS S32750 superduplex stainless steel, Eng. Fail. Anal. 35 (2013) 88–94.
[9] K. Lau, I. Lasa, 3 - corrosion of prestress and post-tension reinforced-concrete bridges, in: A. Poursaee (Ed.), Corrosion of Steel in Concrete Structures, Woodhead Publishing, Oxford, 2016, pp. 37–57.
[10] G.L. Balázs, G. Farkas, T. Kovács, 10 - reinforced and prestressed concrete bridges, in: A. Pipinato (Ed.), Innovative Bridge Design Handbook, second ed., Butterworth-Heinemann, 2022, pp. 267–325.
[11] R.E. Abendroth, R.A. Stuart, D. Yuan, Epoxy-coated and uncoated strand transfer lengths for PC panels, J. Struct. Eng. 123 (5) (1997) 550–560.
[12] F.H. Administration, Methodology for Risk Assessment of PostTensioning Tendons, U.S. Department of Transportation, 2022.
[13] D.A. Bruce, *A Historical Review of the Use of Epoxy Protected Strand for Prestressed Rock Anchors* in *Dam Maintenance and Rehabilitation*, Routledge, London, 2017.
[14] F. Cui, A. Sagues, Exploratory assessment of corrosion behavior of stainless steel clad rebar: Part 1 experimental, Corrosion 62 (2006).
[15] P.G. Deshpande, et al., Corrosion Performance of Polymer-Coated, Metal-Clad, and Other Rebars as Reinforcements in Concrete, 2000.
[16] C. Natarajan, et al., Corrosion protection by coatings on prestressed steel, Corrosion 61 (12) (2005).

[17] J.L. Kepler, D. Darwin, C.E. Locke Jr., Evaluation of Corrosion Protection Methods for Reinforced Concrete Highway Structures, University of Kansas, Kansas, 2000, p. 221.
[18] A. Zomorodian, et al., Anti-corrosion performance of a new silane coating for corrosion protection of AZ31 magnesium alloy in Hank's solution, Surf. Coating. Technol. 206 (21) (2012) 4368–4375.
[19] Z. Chunyan, et al., Ratio of total acidity to pH value of coating bath: a new strategy towards phosphate conversion coatings with optimized corrosion resistance for magnesium alloys, Corrosion Sci. 150 (2019) 279–295.
[20] P. Soroushian, R.-U.-D. Nassar, A.M. Balachandra, Piezo-driven self-healing by electrochemical phenomena, J. Intell. Mater. Syst. Struct. 24 (4) (2013) 441–453.
[21] S. Zhang, N. van Dijk, S. van der Zwaag, A review of self-healing metals: fundamentals, design principles and performance, Acta Metall. Sin. 33 (9) (2020) 1167–1179.
[22] S. An, et al., A review on corrosion-protective extrinsic self-healing: comparison of microcapsule-based systems and those based on core-shell vascular networks, Chem. Eng. J. 344 (2018) 206–220.
[23] J. Wang, et al., Corrosion resistant coating with passive protection and self-healing property based on Fe3O4-MBT nanoparticles, Corrosion Communications 7 (2022) 1–11.
[24] H. Pulikkalparambil, S. Siengchin, J. Parameswaranpillai, Corrosion protective self-healing epoxy resin coatings based on inhibitor and polymeric healing agents encapsulated in organic and inorganic micro and nanocontainers, Nano-Structures & Nano-Objects 16 (2018) 381–395.
[25] X. Liu, et al., Preparation of epoxy microcapsule based self-healing coatings and their behavior, Surf. Coating. Technol. 206 (23) (2012) 4976–4980.
[26] F. Safaei, et al., Single microcapsules containing epoxy healing agent used for development in the fabrication of cost efficient self-healing epoxy coating, Prog. Org. Coating 114 (2018) 40–46.
[27] M. Beiro, et al., Characterisation of barrier properties of organic paints: the zinc phosphate effectiveness, Prog. Org. Coating 46 (2) (2003) 97–106.
[28] G. Blustein, et al., Three generations of inorganic phosphates in solvent and water-borne paints: a synergism case, Appl. Surf. Sci. 252 (5) (2005) 1386–1397.
[29] Y. Shao, et al., The role of a zinc phosphate pigment in the corrosion of scratched epoxy-coated steel, Corrosion Sci. 51 (2) (2009) 371–379.
[30] B. del Amo, et al., Study of the anticorrosive properties of zinc phosphate in vinyl paints, Prog. Org. Coating 33 (1) (1998) 28–35.
[31] J.-M. Hu, et al., Corrosion electrochemical characteristics of red iron oxide pigmented epoxy coatings on aluminum alloys, Corrosion Sci. 47 (11) (2005) 2607–2618.
[32] A. Balachandra, R.-U.-D. Nassar, P. Soroushian, Development and experimental verification of innovative corrosion protection epoxy coatings for steel, Anti-corrosion Methods & Mater. 70 (5) (2023) 294–303.
[33] A.S.f.T.a. Materials, ASTM B117-19 - Standard Practice for Operating Salt Spray (Fog) Apparatus, ASTM, 2019.
[34] A.S.f.T.a. Materials, ASTM A882/A882M - Standard Specification for Filled Epoxy-Coated Seven-Wire Prestressing Steel Strand, ASTM, 2010.
[35] A.S.f.T.a. Materials, ASTM D714-87, Standard Test Method for Evaluating Degree of Blistering of Paints, ASTM, 2000, 2000.
[36] R. Souto, S. Gonzalez, I.C. Rosca, Investigation of the corrosion resistance characteristics of pigments in alkyd coatings on steel, Prog. Org. Coating 43 (2001) 282–285.
[37] J.-T. Zhang, et al., Studies of water transport behavior and impedance models of epoxy-coated metals in NaCl solution by EIS, Prog. Org. Coating 51 (2) (2004) 145–151.
[38] A.S.f.T.a. Materials, ASTM D1654-08, *e1 - Standard Test Method For Evaluation Of Painted Or Coated Specimens Subjected To Corrosive Environments*. 2016, ASTM, 2016.
[39] A.S.f.T.a. Materials, ASTM G20 - Standard Test Method for Chemical Resistance of Pipeline Coatings, ASTM, 2010.
[40] D.-Y. Yoo, et al., Material and bond properties of ultra high performance fiber reinforced concrete with micro steel fibers, Compos. B Eng. 58 (2014) 122–133.
[41] S. Ahmad, et al., Synthesis, characterization, and performance evaluation of hard, anticorrosive coating materials derived from diglycidyl ether of bisphenol A acrylates and methacrylates, J. Appl. Polym. Sci. 95 (3) (2005) 494–501.
[42] M. Kathalewar, A. Sabnis, G. Waghoo, Effect of incorporation of surface treated zinc oxide on non-isocyanate polyurethane based nano-composite coatings, Prog. Org. Coating 76 (9) (2013) 1215–1229.
[43] M. Zhang, et al., Preparation and characterization of fluorescence probe from assembly hydroxyapatite nanocomposite, Nanoscale Res. Lett. 5 (4) (2010) 675–679.
[44] C.C. Lee, F. Mansfeld, Automatic classification of polymer coating quality using artificial neural networks, Corrosion Sci. 41 (3) (1998) 439–461.
[45] J.R. Scully, S.T. Hensley, Lifetime prediction for organic coatings on steel and a magnesium alloy using electrochemical impedance methods, Corrosion 50 (9) (1994).